International Journal of Bioprinting

RESEARCH ARTICLE

Evaluation of surgical fixation methods for the implantation of melt electrowriting-reinforced hyaluronic acid hydrogel composites in porcine cartilage defects

Jonathan H. Galarraga[1], Hannah M. Zlotnick[1,2,3], Ryan C. Locke[2,3], Sachin Gupta[2,3], Natalie L. Fogarty[3], Kendall M. Masada[3], Brendan D. Stoeckl[1,2,3], Lorielle Laforest[3], Miguel Castilho[4,5], Jos Malda[4,6], Riccardo Levato[4,6], James L. Carey[2,3], Robert L. Mauck[1,2,3]*, Jason A. Burdick[1,7]*

[1]Department of Bioengineering, School of Engineering and Applied Sciences, University of Pennsylvania, Philadelphia, PA, USA

[2]Translational Musculoskeletal Research Center, Corporal Michael J. Crescenz VA Medical Center, Philadelphia, PA, USA

[3]Department of Orthopaedic Surgery, McKay Orthopaedic Research Laboratory, University of Pennsylvania, Philadelphia, PA, USA

[4]Department of Orthopaedics, University Medical Center—Utrecht, Utrecht, The Netherlands

[5]Department of Biomedical Engineering, Technical University of Eindhoven, Eindhoven, The Netherlands

[6]Department of Clinical Sciences, Utrecht University, Utrecht, The Netherlands

[7]BioFrontiers Institute and Department of Chemical and Biological Engineering, University of Colorado, Boulder, CO, USA

***Corresponding authors:**
Robert L. Mauck
(lemauck@pennmedicine.upenn.edu)

Jason A. Burdick
(jason.burdick@colorado.edu)

(This article belongs to *Special Issue: Near-field Electrospinning and Melt Electrowriting for Biotechnology and Biomedicine*)

Citation: Galarraga JH, Zlotnick HM, Locke RC, *et al*., 2023, Evaluation of surgical fixation methods for the implantation of melt electrowriting-reinforced hyaluronic acid hydrogel composites in porcine cartilage defects. *Int J Bioprint*, 9(5): 775.
https://doi.org/10.18063/ijb.775

Received: February 15, 2023
Accepted: May 11, 2023
Published Online: June 14, 2023

Abstract

The surgical repair of articular cartilage remains an ongoing challenge in orthopedics. Tissue engineering is a promising approach to treat cartilage defects; however, scaffolds must (i) possess the requisite material properties to support neocartilage formation, (ii) exhibit sufficient mechanical integrity for handling during implantation, and (iii) be reliably fixed within cartilage defects during surgery. In this study, we demonstrate the reinforcement of soft norbornene-modified hyaluronic acid (NorHA) hydrogels via the melt electrowriting (MEW) of polycaprolactone to fabricate composite scaffolds that support encapsulated porcine mesenchymal stromal cell (pMSC, three donors) chondrogenesis and cartilage formation and exhibit mechanical properties suitable for handling during implantation. Thereafter, acellular MEW-NorHA composites or MEW-NorHA composites with encapsulated pMSCs and precultured for 28 days were implanted in full-thickness cartilage defects in porcine knees using either bioresorbable pins or fibrin glue to assess surgical fixation methods. Fixation of composites with either biodegradable pins or fibrin glue ensured implant retention in most cases (80%); however, defects treated with pinned composites exhibited more subchondral bone remodeling and inferior cartilage repair, as evidenced by micro-computed tomography (micro-CT) and safranin O/fast green staining, respectively, when compared to defects treated with glued composites. Interestingly, no differences in repair tissue were observed between acellular and cellularized implants. Additional work is required to assess

the full potential of these scaffolds for cartilage repair. However, these results suggest that future approaches for cartilage repair with MEW-reinforced hydrogels should be carefully evaluated with regard to their fixation approach for construct retention and surrounding cartilage tissue damage.

Keywords: Melt electrowriting; Hydrogel; Cartilage Repair; Mesenchymal Stromal Cells; Fibrin Glue

1. Introduction

A variety of surgical approaches have been developed to treat full-thickness cartilage defects due to trauma and disease, including arthroscopic debridement, microfracture, and autologous chondrocyte implantation (ACI)[1]. Importantly, if cartilage defects are left untreated, they may progress to osteoarthritis (OA), which results in significant pain and joint dysfunction for patients[2]. Unfortunately, these approaches fail to restore healthy cartilage structure and function, as the repair cartilage formed as a result of strategies such as microfracture typically exhibits inferior properties when compared to healthy articular cartilage[3]. However, the success of each of these respective approaches correlates with defect size, which dictates the indication for each procedure[1]. Bone marrow stimulation via subchondral microfracture is widely considered to be the first option for treating relatively small lesions (<2.5 cm^2), with defects ranging between 1 and 2.5 cm^2 responding well to the treatment[1]. However, microfracture has previously demonstrated poor patient outcomes in the treatment of larger defects (≥4 cm^2)[1], which typically must be repaired with osteochondral allografts where available. For intermediate defect sizes (2 cm^2), ACI is typically used to mediate repair[1]; however, ACI is not usually employed for larger defects (≥4 cm^2) since there is typically a limited number of donor cells that can be readily isolated.

In response to the limitations of current approaches for cartilage repair[4,5], a variety of new tissue engineering therapies are being developed, and several have been evaluated for cartilage repair in large animals[6-9]. These have been met with varied success, but highlight the importance of selecting models and time points that best recapitulate human cartilage damage in a clinically relevant manner. To this end, canine, caprine, porcine, and equine models are most commonly used for the investigation of new cartilage repair strategies[10]. Porcine models are often employed as large animal models for cartilage damage because they permit easy operative access to non-load-bearing articular cartilage (i.e., along the femoral trochlea) and possess cartilage with a thickness comparable to human articular cartilage[11]. For example, composite scaffolds consisting of woven polycaprolactone (PCL) and either infilled hydrogels (i.e., self-assembling peptide-based hydrogels and HA hydrogels) or bone marrow aspirate were previously investigated for the treatment of cartilage lesions (4 mm diameter) in Yucatan minipigs[9]. Despite the early observation of scaffold retention in defects at 6 weeks, defects treated with composites performed worse than those treated with microfracture. Similarly, biphasic composites of PCL and cell-laden PEG hydrogel were evaluated in minipig cartilage defects for 6 months; explanted composites resulted in O'Driscoll scores (i.e., histological scoring) that were worse than empty defect controls, and significant bone resorption was observed[6].

One significant challenge in implementing these therapies is the successful fixation and retention of implants within full-thickness cartilage defects[7,12,13]. A range of approaches have been investigated for implant fixation[14], including press-fitting, suturing with an overlaying periosteal flap, application of fibrin glue/sealant, and the use of bone anchors to integrate implants with the underlying bone, among others. While simply press-fitting an implant may be appropriate for osteochondral defects or instances in which full-thickness cartilage defects are surrounded by healthy, thick cartilage[15], oftentimes chondral-only samples are dislodged from defects due to the complex loads experienced within the joint[14,16]. Fibrin glue has similarly been combined with press-fitting of implants, but only marginally improved the fixation strength and retention of implants[16-18]. Unfortunately, suturing of periosteal flaps to secure implants within defects leads to the loss of chondrocytes and extracellular matrix (ECM) at the local suture site, as well as the formation of fissures reminiscent of partial-thickness defects[19]. Bone anchors have been shown to ensure the retention of implants within defects more reliably[9], but they often lead to underlying subchondral bone remodeling or voids[18,20]. A recent study evaluated biphasic scaffolds composed of hydroxyapatite and PCL microfiber meshes fabricated via melt electrowriting (MEW) in an equine osteochondral damage model. Six months after implantation, minimal cartilaginous ECM was observed in the chondral phase of implants, while micro-computed tomography (micro-CT) results showed the collapse of bone anchors used to fix the implants within defects, potentially due to improper design and fixation[7]. Generally, both the cartilage defect size and geometry, as well as the properties of the implant itself must be considered when selecting the optimal fixation method for scaffolds.

In our previous work, composites of norbornene-modified hyaluronic acid (NorHA) hydrogels mechanically

reinforced with melt electrowritten PCL supported juvenile bovine mesenchymal stromal cell (MSC) chondrogenesis and neocartilage formation while also achieving high initial construct mechanical properties[21]. The compressive moduli and biochemical content achieved in these MEW-NorHA composites *in vitro* approached that of native tissues and, taken together with their ability to integrate with native articular cartilage *ex vivo*, motivated additional exploration of their therapeutic potential in a clinically-relevant model of cartilage damage. Thus, the aims of this study were (i) to explore adult porcine MSC behavior within MEW-NorHA composites and (ii) to elucidate how surgical fixation methods influence the efficacy of these composites in a porcine model of cartilage damage.

2. Materials and methods

2.1. Materials

Sodium hyaluronic acid was obtained from Lifecore Biomedical (Chaska, MN), and lithium phenyl-2,4,6-trimethylbenzoylphosphinate (LAP) was obtained from Colorado Photopolymer Solutions (Boulder, CO). Unless otherwise specified, all other reagents and materials were purchased from Sigma-Aldrich (St. Louis, MO).

2.2. MEW-NorHA composite fabrication and cell culture

First, PCL (Purasorb PC 12, Corbion Inc., Gorinchem, Netherlands) box-structured MEW meshes (diameter ~4 mm, height ~1 mm, 400 μm fiber interspacing) were fabricated as previously reported[22]. In short, a custom-built MEW device was used to heat PCL to 90°C, creating a polymer melt (heating system from TR 400, HKEtec, Germany) that could then be fed through an electrically charged 23G spinneret (power supply from Heinzinger Electronic GmbH, Rosenheim, Germany). PCL polymer melt fibers (~20 μm) were then layered in a 90° lay-down pattern onto a computer-controlled translating collector (acceleration voltage = 5.5 kV, spinning gap = 3.3 mm, E = 1.3 kV mm^{-1}) to obtain MEW scaffolds. Finally, disc-shaped scaffolds were extracted from initially fabricated sheets of MEW scaffolds using 4 mm biopsy punches.

NorHA was synthesized, as previously described, via benzotriazole-1-yl-oxy-tris-(dimethylamino)-phosphonium hexafluorophosphate (BOP) coupling[23]. Briefly, sodium hyaluronic acid was first converted into its tetrabutylammonium salt form (HA-TBA), which was then dissolved in anhydrous dimethyl sulfoxide (DMSO). HA-TBA was then reacted with 5-norbornene-2-methylamine in the presence of BOP under inert nitrogen for 2 h at room temperature. The reaction solution was then quenched with the addition of cold distilled water. To purify the crude product, the solution was dialyzed (8–10 total days), and any precipitates were removed via filtration. The degree of modification (~22%) was quantified via ^{1}H-NMR spectroscopy (Bruker Neo400 360 MHz) to confirm the successful conjugation of norbornene groups to the HA backbone. After synthesis, NorHA was dissolved in phosphate-buffered saline (PBS) with LAP photoinitiator (0.05%) and dithiothreitol (DTT) crosslinker (0.54 mM) to obtain a macromer precursor solution.

The prepared macromer solutions were pipetted into the box-structured PCL MEW meshes with or without porcine MSCs (pMSCs, P1, 20×10^6 cells/mL) and irradiated with blue light (400–500 nm, Omnicure lamp with an affixed collimator, I = 10 mW/cm^2) for 5 min to obtain composites similar to those investigated in our previous studies (i.e., 400 μm interfiber spacing within PCL MEW meshes and NorHA hydrogels with a compressive modulus of ~2 kPa)[21]. Porcine MSCs were isolated from bone marrow aspirates of three adult Yucatan minipigs (12–14 months old; Sinclair Research, Auxvasse, MO) via plastic adherence and cultured in Dulbecco's modified eagle medium (DMEM) supplemented with 10% fetal bovine serum (FBS) and 1% penicillin/streptomycin (P/S). After fabrication, composites were cultured in chondrogenic media (1% insulin–transferrin–selenium solution, 2.5 μg/mL amphotericin B, 1×10^{-3} M sodium pyruvate, 50 μg/mL ascorbic acid 2-phosphate, 40 μg/mL L-proline, 1×10^{-7} M dexamethasone, and 10 ng/mL TGF-β3) for up to 28 days.

2.3. Composite characterization

Live/Dead staining with calcein AM and ethidium homodimer was first performed in accordance with the manufacturer's instructions (Invitrogen) after 7 days of culture in chondrogenic media to evaluate encapsulated pMSC cell viability. Cell viability was quantified using ImageJ software as the number of live cells per total cells within images acquired via epifluorescence microscopy ($n \geq 3$ hydrogels, 9 images per sample).

After culture in chondrogenic media for 28 days, constructs were evaluated for biomechanical and biochemical properties. First, the compressive moduli of composites were determined via unconfined, uniaxial compressive testing with a constant loading rate of 0.2 N/min (Q800 DMA, TA Instruments). The modulus was quantified as the slope of the stress–strain curves between 10% and 20% strain. Samples were then minced and digested via incubation with papain and hyaluronidase overnight at 60°C[21]. Sulfated glycosaminoglycan (sGAG) content, collagen (COL) content, and DNA content were determined via the dimethylmethylene blue assay, the hydroxyproline (OHP) assay (Abcam Hydroxyproline Assay Kit, ab222941), and the Picogreen dsDNA assay, respectively[24]. Separate samples were processed for

histology through fixation (10% buffered formalin), paraffin embedding, and sectioning (5 μm). Alcian blue staining (1%, pH 1.0, Newcomer Supply) and immunohistochemistry for type I collagen (COL I, mouse monoclonal anti-collagen type I antibody, Millipore Sigma) and type II collagen (COL II, mouse monoclonal anti-collagen type II antibody, Developmental Studies Hybridoma Bank) were then performed as previously described[21]. The mean staining intensities of sGAG, COL I, and COL II in composites were quantified using ImageJ software[25].

2.4. Animal procedures and stifle joint surgery

Skeletally mature (12–14-month-old at time of surgery) castrated male Yucatan minipigs were acquired (Sinclair Bioresources, Auxvasse, MO) and used to evaluate surgical fixation methods for the implantation of MEW-NorHA composites in cartilage defects *in vivo*. All animal procedures were approved by the Institutional Animal Care and Use Committee (IACUC) at the University of Pennsylvania. Unilateral stifle joint surgeries were performed on the right hind limb of each animal as previously described[16,26,27]. Briefly, four full-thickness chondral defects were created in the trochlear groove (two proximal and distal medial defects and two proximal and distal lateral defects) using a 4 mm biopsy punch and a curette to excise cartilage within the bounds of the scored defect while ensuring the underlying subchondral bone was not damaged. Nine total animals were used (some defects were part of an alternate study). In two animals, post-operative lateral patellar luxation was observed 3 weeks after surgery, and these were excluded from the study. Luxation was likely due to recovery-related complications and/or patellar luxation accompanied by urticaria and incisional dehiscence consistent with a previously reported case of suture hypersensitivity in a Yucatan minipig[28].

Four groups (n = 4–6 implants/group) were assessed, including acellular composites or composites containing pMSCs that were precultured for 28 days and implanted with either poly(L-lactide-co-D,L-lactide) (PLDLLA) pins (Aesculap FR736, Center Valley, PA) or fibrin glue (Tisseel, Baxter), as previously reported[16]. Composites were pinned by press-fitting into the defects, creating a pilot hole through the implant and into the subchondral bone, placing a 3-pronged fixation guide (Aesculap FR720, Center Valley, PA) on top of the composites, and then inserting the pins into the pilot holes. In two animals, an additional fifth defect was introduced on the lateral side of the femoral trochlea to replace medial distal defects in which insufficient fixation of implants with pins was initially achieved (i.e., poor seating of composites within the created defect and misaligned pinning at the time of fixation). Each of these additional, lateral distal defects was evaluated in lieu of the medial distal defects in all the performed analyses. To fix composites within defects using fibrin glue (Tisseel), the fibrin glue was first applied to the underlying subchondral bone, the composites were press-fit into the defects and manually held in place for 3 min via application of force with a spatula and a surgical curette, and additional fibrin glue was then applied along the top of the composite surface.

After composite fixation, the patella was relocated, all instruments and retractors were removed, and the knee was then ranged to ensure that the patella was stable. The joint capsule was then closed with 0 Vicryl interrupted sutures, the subcutaneous tissue layer was closed with 2-0 Vicryl simple interrupted sutures, and the skin layer was closed with a 3-0 monocryl running suture (all sutures were procured from Ethicon, Raritan, NJ). All animals received post-operative analgesia, antibiotics, and anti-inflammatories, with unrestricted cage activity permitted 2 to 3 h after recovery from anesthesia.

2.5. Arthroscopy, micro-CT, and histological evaluation of cartilage defects

Twelve weeks after cartilage defect creation, animals were euthanized, and the stifle joints were retrieved for post-mortem analyses. Dry arthroscopy was first performed to visualize the cartilage defects *in situ* using an adapted protocol[16]. A 1 cm vertical incision was made to establish a medial subpatellar arthroscopic portal, which allowed for the placement of a trocar and arthroscopic probe within the medial aspect of the stifle joint. Images of each defect were then taken to qualitatively evaluate the retention of pinned or glued composites, the smoothness of formed repair cartilage, and the integration of repair cartilage with the surrounding tissue[29]. The stifle joint was dissected, and cartilage defects along the trochlear groove were macroscopically assessed to qualitatively determine the retention of implants and the quality of repair cartilage formed in defects[30].

To visualize any subchondral bone remodeling or bone resorption that occurred during the 12-week course, explanted cartilage defects (and healthy tissue controls) were imaged via micro-CT as previously described[31]. Osteochondral samples were incubated in Lugol's solution overnight at room temperature and then imaged using a Scanco MicroCT 45 system (Scanco Medical, Southeastern, PA; exposure: 600 ms, voltage: 55 kVp, isotropic voxel size: 10 μm), with cross-sectional and top-down images of samples acquired via DragonFly software (Object Research Systems, Montreal, Canada). After micro-CT imaging, samples were fixed (10% formalin, 24–48 h incubation overnight at 4°C) and decalcified via incubation in Formical-2000 for 4 weeks (solution changed

weekly). Thereafter, samples were embedded in paraffin, sectioned (8 μm), and stained with either picrosirius red to visualize collagen content or safranin O/fast green to visualize proteoglycan and collagen content, respectively, within the repair cartilage and the underlying subchondral bone. The ICRS II Histological Assessment Scale ($n \geq 12$ replicates) was employed to assess safranin O/fast green-stained samples, with scores ranging from 0% to 100% (worst–best) averaged across three blinded reviewers[32]. These blinded reviewers also qualitatively selected the best and worst micro-CT and picrosirius red images obtained for each investigated experimental group.

2.6. Indentation testing of composites and repair cartilage

To evaluate the mechanical properties of repair cartilage 12 weeks after defect creation, creep indentation testing was performed as previously described using an Instron 5948 Universal Testing System (Instron Inc., Norwood, MA) with an affixed 1 mm diameter spherical indenter[33]. Since large deformations during physiologic creep testing may significantly alter the local compositional characteristics of immature tissue constructs (i.e., acellular composites), lower loads were employed during all indentation testing to ensure the accurate quantification of mechanical properties[34]. Generally, a load of 0.1 N was applied to all samples at a loading rate of 0.1 N/s and then held for 900 s (after the load setpoint was reached) while the creep displacement was measured. Prior to testing, osteochondral samples were first fixed into place within a low-melting temperature bismuth alloy to secure samples while maintaining the cartilage defect surface upright. Samples were then submerged in PBS and positioned under the indenter setup using a custom XY positioning stage and a goniometer to ensure that the cartilage surface was perpendicular to the indenter. Repair cartilage within the center of defect samples (or directly adjacent to pins in instances where pins were still visible and exposed on the cartilage surface) was then indented. After osteochondral sample fixation and decalcification, defects were cut along their midplane to determine the thickness of cartilage samples. The compressive modulus, tensile modulus, and permeability of all indented samples were then quantified by fitting the collected creep data to a Hertzian biphasic model[35].

2.7. Statistical analysis

All statistical analyses were performed using GraphPad Prism 9 software, with data reported as mean ± standard deviation and significance for all performed analyses determined at $p < 0.05$. One-way analyses of variance (ANOVAs) were performed with Tukey's honestly significant difference (HSD) *post-hoc* testing to compare functional outcomes between porcine donors, cell viability across cultured composites, and the resultant mechanical properties for the experimental groups investigated in the porcine model.

3. Results and discussion

3.1. Composite fabrication and pMSC donor screen for chondrogenic potential

MEW-NorHA composites were fabricated by first heating PCL into a polymer melt that is amenable to melt electrowriting using a custom-built device[22]. As the PCL polymer melt is fed through the spinneret, a high-voltage source is applied, leading to the formation of an electrically charged polymer melt fiber. The deposition of these fibers is then controlled using a translating collector, allowing for the layer-by-layer fabrication of mesh structures (Figure 1A). More specifically, MEW scaffolds were formed by depositing polymer melt fibers in a 90° lay-down pattern, with 400 μm interfiber spacing between parallel fibers (Figure 1B). PCL MEW scaffolds could then be combined with acellular or pMSC-laden NorHA hydrogels to form MEW-NorHA composites (Figure 1C).

To evaluate the retention of MEW-NorHA hydrogel composites within full-thickness cartilage defects, it was first necessary to validate that the composites support the chondrogenesis of adult porcine MSCs toward the formation of neocartilage. Adult pMSCs were selected as an allogenic cell source to mitigate any potential immune responses upon implantation in minipigs[36]. Isolated pMSCs were age-matched to the host animals (12–14 months) to ensure that they best represented the clinically-relevant scenario in which autologous cells are sourced and used within implants. Moreover, skeletally mature minipigs were selected as host animals to mitigate subchondral bone remodeling, which has been previously reported in juvenile minipigs[27], and to recapitulate the higher loading environment that is normally experienced in adults with cartilage defects. NorHA macromer along with dithiol crosslinker (DTT) and photoinitiator (LAP) were mixed with pMSCs to form a suspension composed of hydrogel precursors and cells that could be readily filled into the interstitial spaces of the fabricated MEW scaffolds. Thereafter, exposure to collimated blue light initiated the thiol-ene crosslinking of pMSC-laden hydrogels within MEW scaffolds (Figure 2A). The process and materials employed to form these composites were cytocompatible, as evidenced by Live/Dead staining after culturing composites for 7 days (Figure 2B). Importantly, relatively high cell viabilities (~80%) of the encapsulated pMSCs were observed across three different porcine donors (Donors 1, 2, and 3), suggesting that long-term culture of pMSCs within MEW-NorHA composites is feasible, irrespective of donor source (Figure 2C). In addition, the

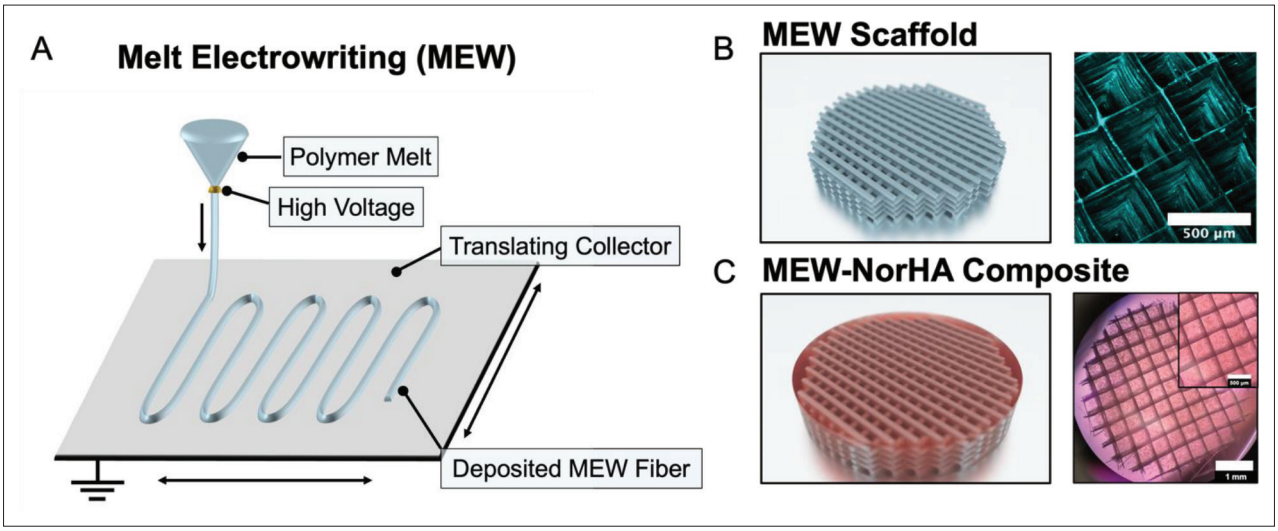

Figure 1. Fabrication of MEW-NorHA composites. (A) Overview of the melt electrowriting (MEW) of polycaprolactone (PCL) microfibers to form MEW scaffolds. (B) (Left) Schematic of MEW scaffolds formed via deposition of overlaying, perpendicular MEW fibers with 400 μm interfiber spacing, and (right) representative micrograph of the MEW scaffold (cyan). (C) (Left) Schematic of the MEW-NorHA composites used to evaluate adult porcine mesenchymal stromal cells (pMSCs) sourced from three porcine donors and (right) representative images of MEW-NorHA composites containing encapsulated pMSCs during culture.

crosslinking chemistry used to form NorHA hydrogels and MEW-NorHA composites is hydrolytically stable, such that long-term culture may be performed *in vitro* without loss of construct stability[37].

Since donor variability is known to influence human MSC properties, such as proliferation and differentiation[38], pMSCs from three prospective porcine donors were screened to identify a cell source with the requisite chondrogenic potential to form neocartilage when cultured in chondrogenic media for 28 days (Figure 3). Given the age of the encapsulated adult pMSCs, it was expected that the mechanical properties and relative amounts of cartilaginous ECM components observed in these composites would be inferior to those previously reported in composites containing juvenile bovine MSCs; however, increases in the compressive moduli of pMSC-laden composites were still observed over 28 days when compared to acellular composite controls (~100 kPa)[21].

Minimal differences were observed across the donors with respect to the compressive moduli (~160 kPa) of cultured composites (Figure 3). However, the DNA content of composites cultured with pMSCs from Donor 3 was significantly higher than that of composites containing pMSCs from Donor 2 despite all the cell-laden composites being fabricated with the same density of encapsulated cells. This suggests that cells from Donor 3 may have had an innately higher proliferative capacity. This data is qualitatively corroborated by the observation of faster proliferation for Donor 3 cells compared to other donors (all plated on tissue culture plastic at a density of 6.67×10^3 cells/cm^2, data not shown). In addition, pMSCs isolated from Donor 3 and encapsulated in composites led to neotissue with significantly higher sulfated glycosaminoglycan contents than composites produced from Donor 1 or 2 (Figure 3). Composites containing cells sourced from Donor 3 also possessed higher average collagen content after culture (25.1 ± 9.5 μg/construct) compared to composites containing cells sourced from Donor 1 (21.1 ± 4.0 μg/construct) or Donor 2 (16.9 ± 3.3 μg/construct).

Evaluation of these composites via histology and immunohistochemistry also demonstrated that composites containing cells from Donors 1 and 3 stained more intensely for sGAG and type I collagen (COL I) than composites containing cells from Donor 2 (Figure 4). However, the morphology of the encapsulated pMSCs, the relative distribution and organization of ECM, and the overall staining intensity were qualitatively comparable across all donors (Figure 4). In addition, relatively intense type II collagen (COL II) staining was observed in the pericellular space of encapsulated cells across all the samples, consistent with previously reported staining in NorHA hydrogels containing bovine MSCs[23]. Based on these results, Donor 3 was selected as the primary allogeneic cell source for all the cell-laden composites fabricated and cultured for implantation *in vivo* to maximize the chondrogenic potential of the precultured composite implants.

3.2. Construct implantation

After screening porcine donors, we next sought to evaluate the fixation of MEW-NorHA composites *in vivo* using a porcine model of full-thickness cartilage defects (Figure 5A)

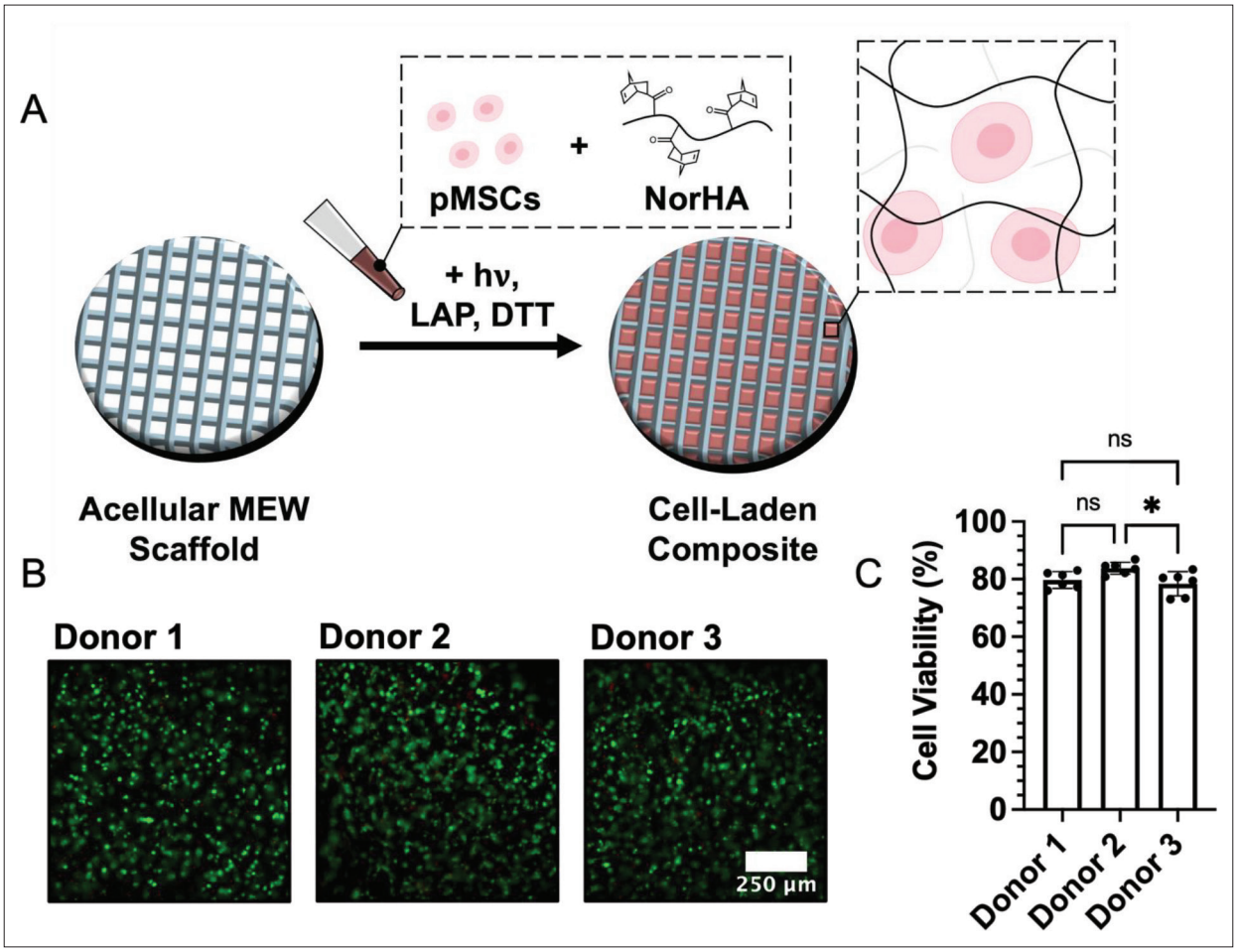

Figure 2. Encapsulation of pMSCs within MEW-NorHA composites. (A) Schematic overview of the encapsulation of pMSCs within MEW-NorHA composites. Cells are suspended in NorHA macromer, which is then infilled into MEW meshes and crosslinked via light-mediated (hν) thiol-ene crosslinking in the presence of LAP photoinitiator and DTT crosslinker. (B) Live/Dead staining and representative micrographs of pMSC-laden composites containing cells sourced from three different porcine donors and cultured for 7 days in chondrogenic media. (C) Quantification of the cell viability within composites 7 days after pMSC encapsulation. $n = 6$, one-way ANOVA with Tukey's HSD *post-hoc* test, $^*p < 0.05$, ns = not significant. DTT: dithiothreitol; LAP: lithium phenyl-2,4,6-trimethylbenzoylphosphinate.

[10]. Cartilage defects were created along the femoral trochlea of Yucatan minipigs to investigate both the retention and performance of implanted acellular and precultured (i.e., culture for 28 days in chondrogenic media) composites. To mitigate the potential influence of defect location on the performance of different experimental groups, treatment location was randomized across all the performed surgeries. Adult animals were selected over skeletally immature animals to better recapitulate the patient populations that develop full-thickness cartilage defects and to mitigate the degree of subchondral bone remodeling that occurs with initial cartilage defect creation[39].

Two distinct fixation methods were investigated to identify how best to implant MEW-NorHA composites within cartilage defects: (i) pinning of composites to the underlying subchondral bone with bioresorbable PLDLLA pins, which degrade on the order of months, and (ii) fixation with fibrin glue (Figure 5B and C). While the former fixation method has been previously shown to retain nanofibrous HA-based scaffolds within full-thickness porcine defects, it is also associated with appreciable subchondral bone remodeling[16]. Alternatively, past results suggest that subchondral bone remodeling is attenuated with the use of fibrin glue[16] but that the retention of implants within defects is not significantly improved when compared to press-fitting alone[17]. Given the previously reported advantages and limitations of these respective approaches, this study aimed to identify the fixation method most appropriate for use with these MEW-NorHA composites.

Unilateral stifle joint surgeries were performed and treated with pinned acellular composites ("Acellular+Pin,"

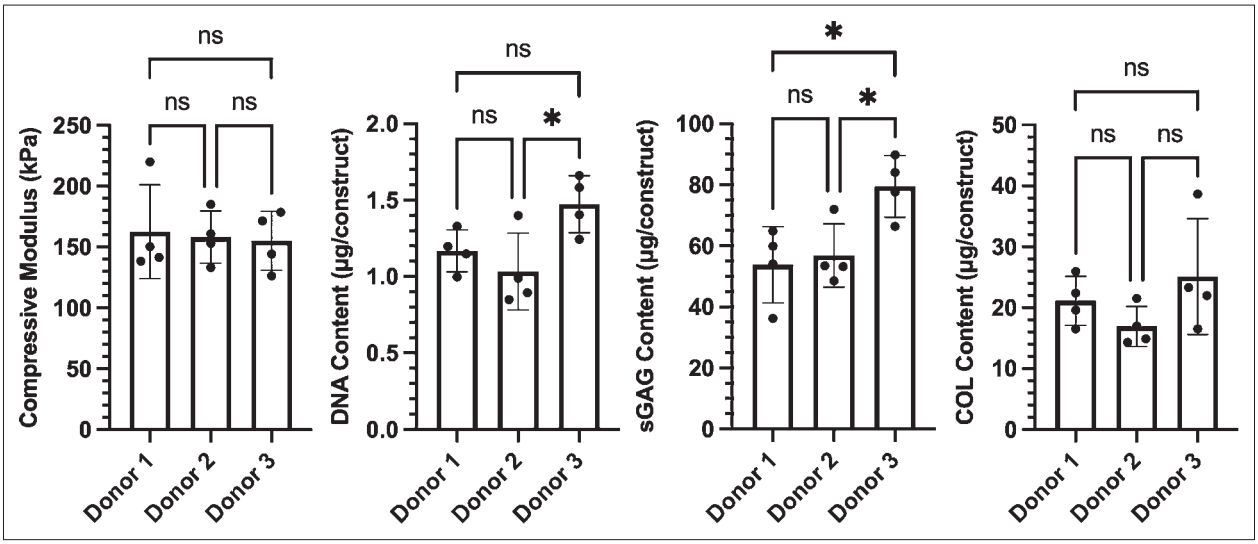

Figure 3. *In vitro* screening of pMSC donors. (Left to right) Compressive modulus and biochemical contents (DNA, sulfated glycosaminoglycan (sGAG), and collagen (COL) contents) of composites containing encapsulated adult pMSCs from 3 donors and cultured for 28 days in chondrogenic media. $n = 4$, one-way ANOVA with Tukey's HSD *post-hoc* test, $^*p < 0.05$, ns = not significant.

$n = 6$), pinned precultured composites ("Precultured+Pin," $n = 4$), glued acellular composites ("Acellular+FG," $n = 4$), or glued precultured composites ("Precultured+FG," $n = 4$). Both acellular and cell-laden composites were implanted in defects to characterize any potential improvements in resultant repair cartilage due to pMSC preculture and neocartilage formation. Twelve weeks after the initial defect formation and treatment, repair cartilage within defects was evaluated via arthroscopy, gross observation, micro-CT, histology, and mechanical testing (Figure 5).

Across all the surgeries in which precultured composites were implanted and explanted, the viability of implants was first investigated via Live/Dead staining of similarly fabricated constructs (same cell and material batch, fabricated at the same time) after the first 7 days of culture in chondrogenic media. Importantly, no differences in cell viability (~79.4% ± 3.0%, $n = 21$) were observed across precultured composites prepared for separate surgeries. In addition, the cell viability observed across all these samples was consistent with that previously observed in our donor screening study (Figure 2C).

3.3. Evaluation of fixation methods and repair cartilage formation

To characterize the presence of implants and the healing response within cartilage defects 12 weeks after surgery, nascent repair cartilage was first assessed via arthroscopy (Figure 6)[29,40]. Although the appearance of defects and repair cartilage varied across animals, a number of features were conserved within each of the treatment groups. Within defects that were generally filled, the repair cartilage exhibited a smooth surface and intimate integration along the border of the defect, albeit with some fibrillation at the defect interface.

Given the size of the created defects (~0.13 cm^2), these observations are consistent with the short-term repair outcomes seen clinically for defects <4 cm^2 that are treated with microfracture[41]. However, some pinned and glued composites also exhibited heterogeneous and incomplete defect filling, with more apparent fissures along the defect border in defects treated with pinned composites. The appearance of repaired cartilage in defects treated with pinned acellular and precultured composites varied. In some instances, damage to the subchondral bone and adjacent cartilage was evident, while in other examples, repaired tissue adjacent to the pin was opaque and level with the adjacent tissue[30]. While glued composites resulted in similarly heterogeneous repair cartilage, in more instances, glued composites facilitated complete defect filling and the formation of smooth cartilage that integrated with the surrounding tissue.

Macroscopic observation of the femoral trochlea corroborated the trends observed via arthroscopy. Interestingly, 8 of the 10 defects treated with pinned composites contained a visible pinhead after explanting the femoral trochlea; although it is expected that the pin would be retained within all defects after 12 weeks based on their previously reported degradation behavior, a 75% success rate of implant fixation was also previously reported with the use of these pins in the same animal model[16]. Although unlikely, retention of implants within the two defects where the pin could not be readily seen may still have been achieved. Given that at least one instance of pin

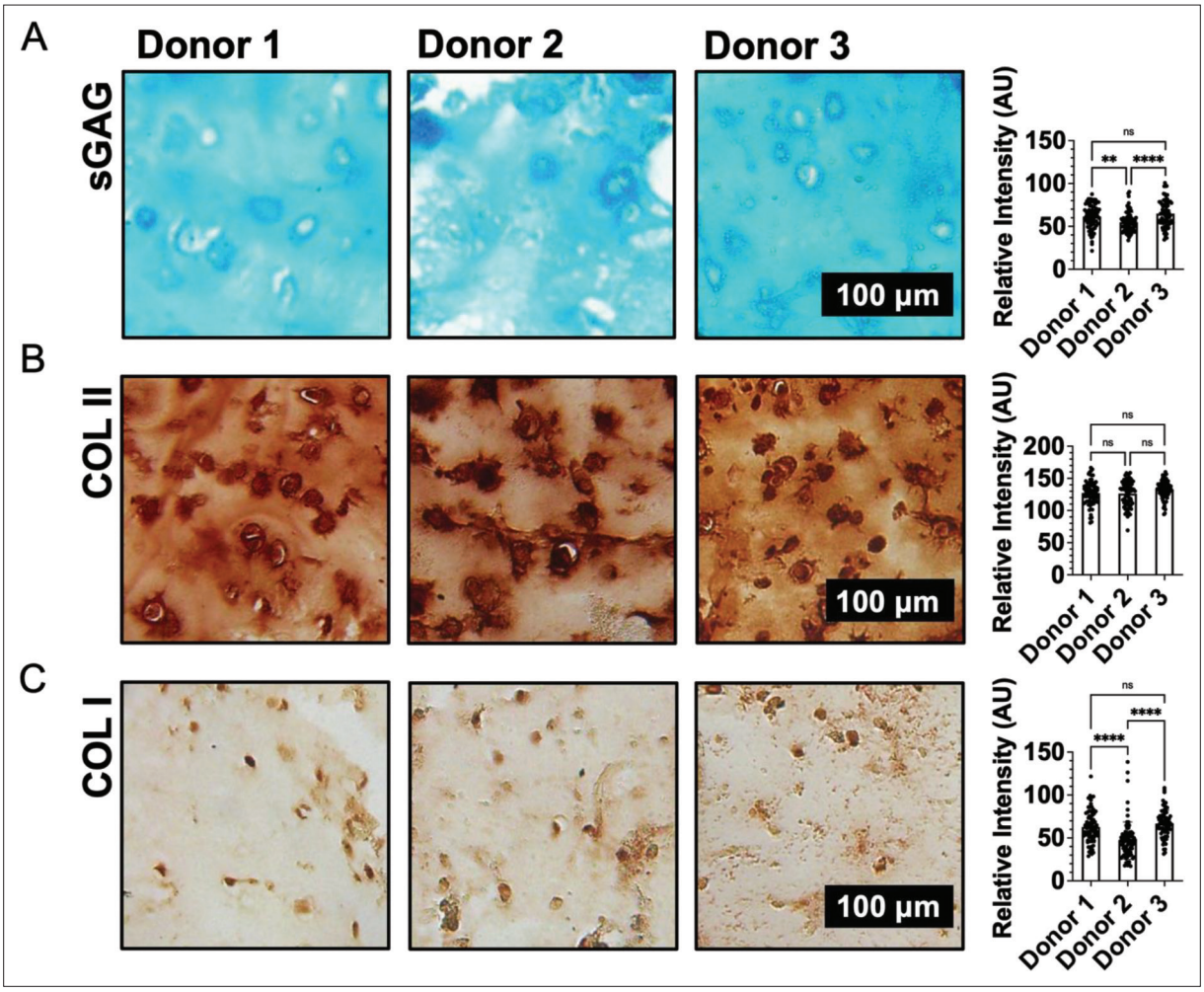

Figure 4. ECM staining of composites across pMSC donors. After 28 days of culture in chondrogenic media, ECM within composites containing encapsulated pMSCs from three porcine donors is visualized via (A) alcian blue staining (for sulfated glycosaminoglycans, sGAG), (B) type II collagen (COL II) immunohistochemistry, and (C) type I collagen (COL I) immunohistochemistry. (A–C) Representative images (left) and quantification of staining intensity (right) to characterize (A) sGAG, (B) COL II, and (C) COL I distribution and organization for three porcine donors. $n = 81$ images, 9 sections, 3 composites; one-way ANOVA with Tukey's HSD *post-hoc* test, $^{**}p < 0.01$, $^{****}p < 0.0001$, ns = not significant.

failure was observed during implantation, it is possible that the pin head may have translocated away from the defect post-operatively. Alternatively, the formation of repair cartilage around and/or above the pin could obscure the presence of underlying pins. For example, pinheads were observed in both lateral defects in one animal much further away from the articular surface (i.e., deeper) than in other samples.

Generally, macroscopic visualization of the trochlea and arthroscopic imaging revealed that the volume of the pin used to fix composites qualitatively impeded the complete filling of defects containing acellular or precultured composites (Figure 6). Moreover, the potential contraction of composites upon formation of pilot holes or the application of the fixation guide (for the insertion of pins through composites and into the subchondral bone) may have perturbed the composite–native tissue interface, further influencing defect fill and repair cartilage integration. Improved defect fill and macroscopic appearance were observed for composites fixed within defects using fibrin glue in lieu of pins; however, at least one defect appeared to be entirely empty (lateral proximal defect) (Figure 6). Specifically, both acellular and precultured composites implanted using fibrin glue exhibited instances where complete defect fill was achieved, and a homogenous, smooth cartilage surface was observed; in parallel, other defects were partially filled at lesser depths with more apparent fissures[30]. Prior observations for implants in ponies showed that fibrin was insufficient to fix chondral implants, which indicates that the species, as well as the implant location, must be considered[12].

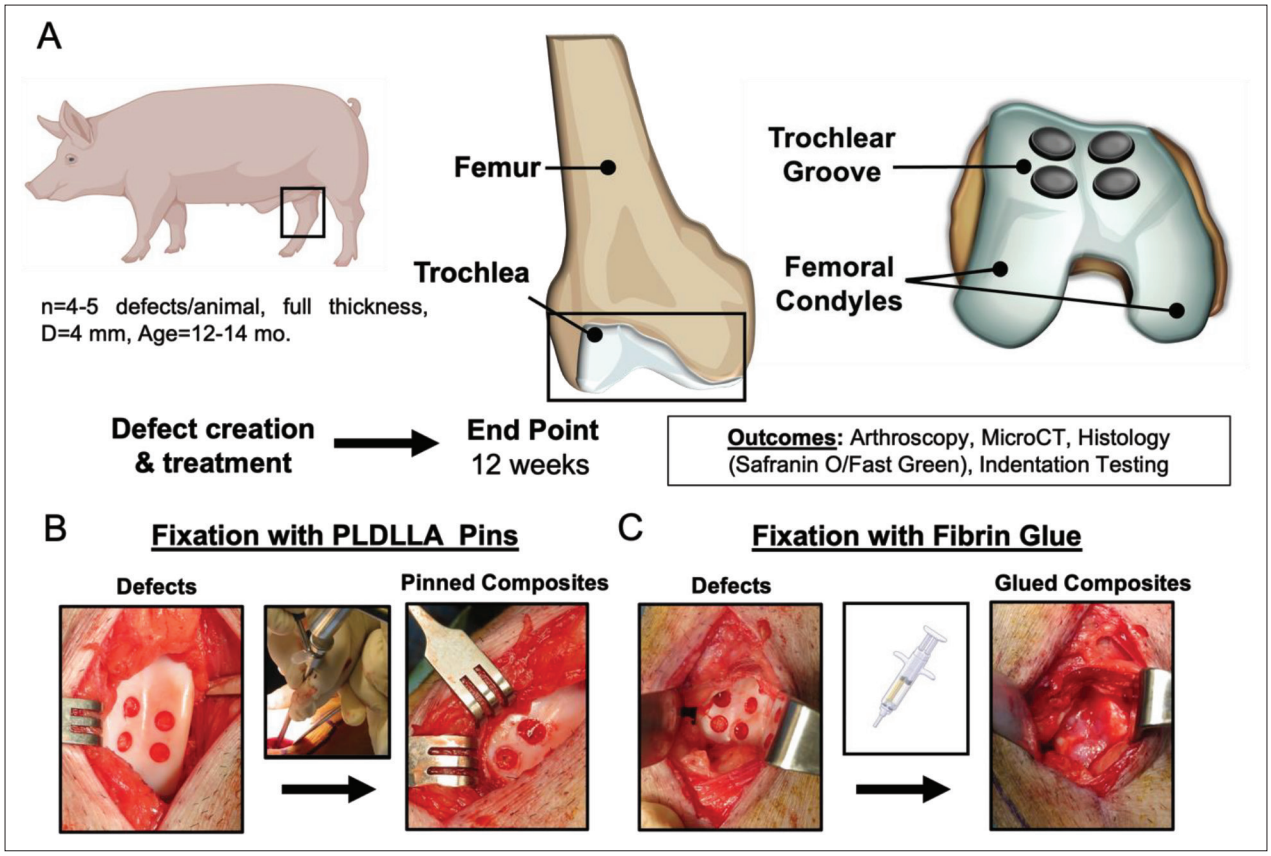

Figure 5. Study design to evaluate MEW-NorHA composite fixation in a porcine model of articular cartilage repair. (A) Full-thickness cartilage defects are created along the trochlear groove of the patellofemoral joint (right, hind stifle joint). Defects are then filled with either acellular or precultured (chondrogenic media, Donor 3 pMSCs, 28 days) MEW-NorHA composites. Twelve weeks after implantation, the retention of implants and the quality of repair cartilage within each of these respective defects were evaluated via arthroscopic imaging, micro-CT, histology, and mechanical testing. To ensure that implants are retained within the created cartilage defects, composites are fixed with either (B) bioresorbable pins (PLDLLA) or (C) fibrin glue sealant. (B–C) Representative images of defects formed along the trochlear groove (left) and composites fixed with either (B) pins or (C) fibrin glue (right).

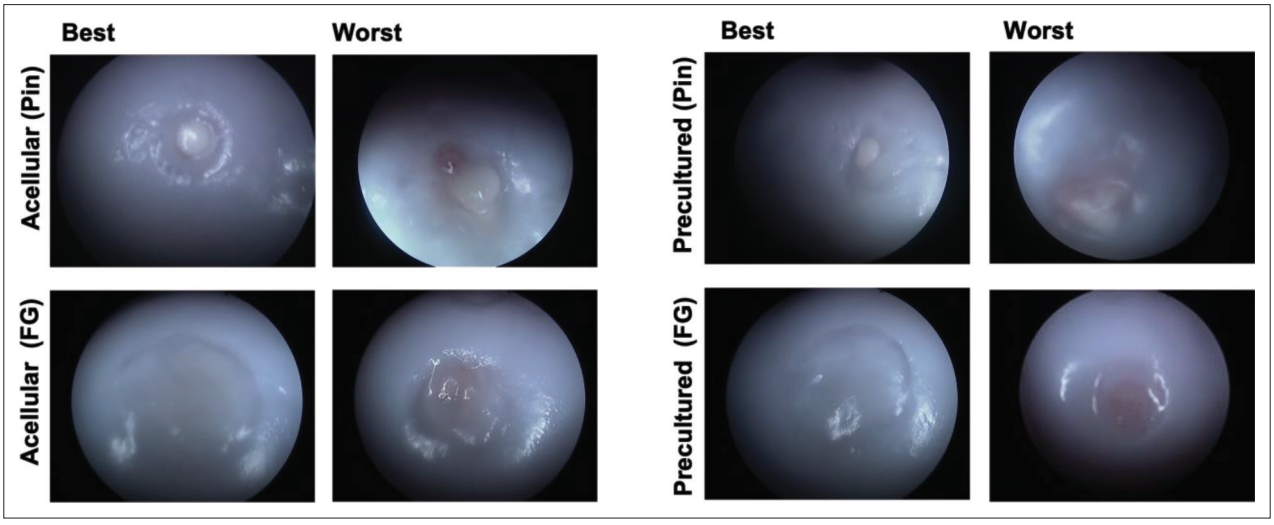

Figure 6. Arthroscopic evaluation of repair cartilage. Representative arthroscopy images of repair cartilage corresponding to each of the respective experimental groups 12 weeks after composite implantation. FG: fibrin glue.

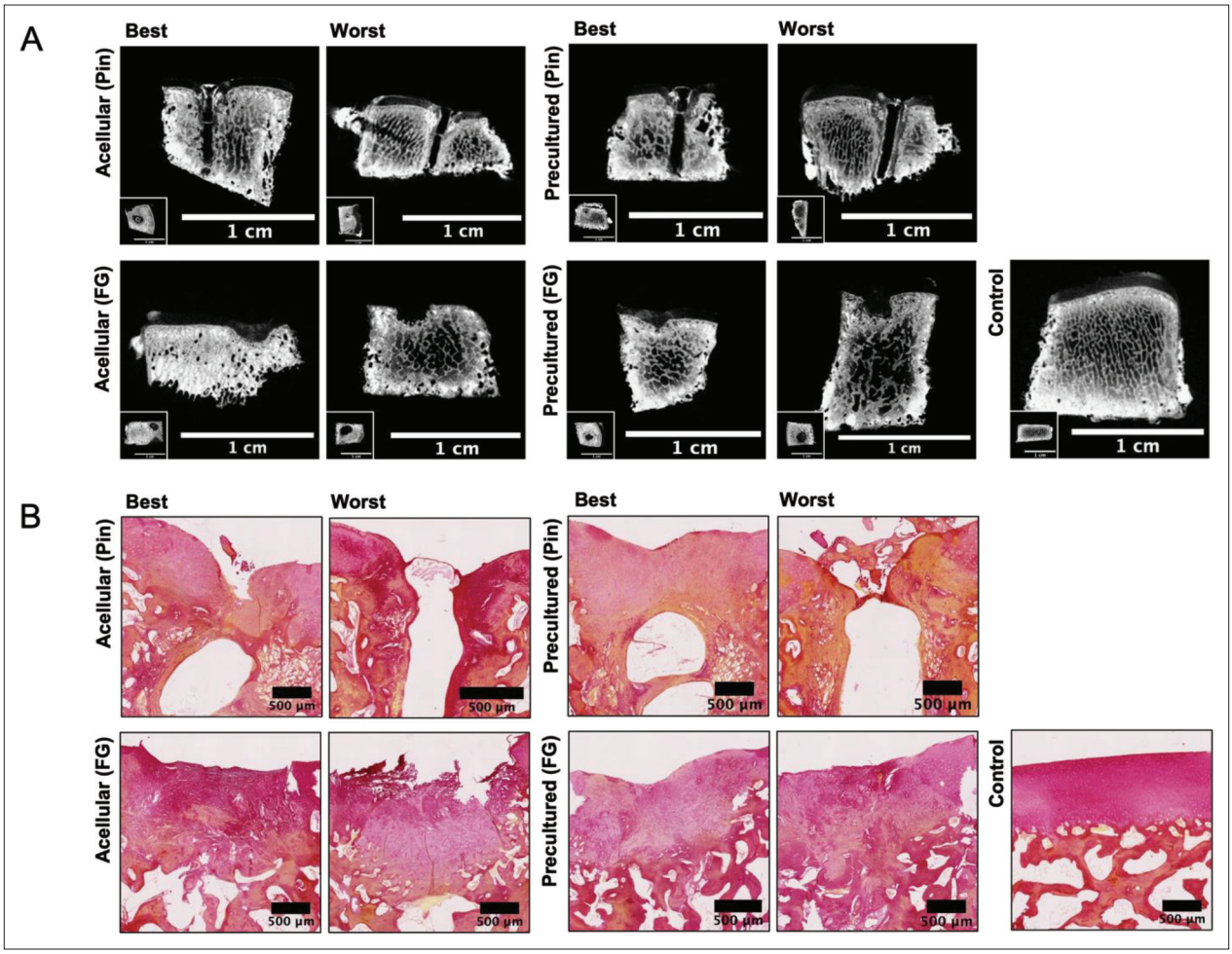

Figure 7. Evaluation of implant fixation methods via micro-CT and picrosirius red staining. (A) Micro-CT scans of cartilage defects and underlying subchondral bone, with representative cross-sectional images 12 weeks after composite implantation shown. Insets show the top-down view for each defect. Scale bars = 1 cm. (B) Picrosirius red staining of repair cartilage, with representative cross-sectional images showing the center of cartilage defects for each of the respective experimental groups 12 weeks after composite implantation. Scale bars = 500 µm. Control osteochondral samples are isolated from the most distal portion of the trochlea for qualitative comparisons. FG: fibrin glue.

Micro-CT was performed on all the cartilage defects to qualitatively assess the relative amount of bone resorption associated with each of the respective treatment groups (Figure 7A). To this end, control osteochondral samples (i.e., healthy tissue) were also isolated from the most distal portion of the trochlea to identify any potential subchondral bone remodeling in treated defects. Subchondral bone remodeling may compromise the long-term stability of any repair cartilage formed in the overlaying defect or alternatively give rise to differential osteochondral loading, leading to the progression of OA[42]. While some degree of bone resorption was qualitatively observed across all experimental groups, bone resorption appeared more pronounced in defects treated with pinned composites. In addition, micro-CT confirmed the presence of the biodegradable pins in defects treated with pinned composites, further corroborating both that the pins did not completely degrade over 12 weeks *in vivo* and that the pinheads, perhaps due to onset of degradation, encompassed an appreciable amount of the overall defect surface area. While this might suggest that there is a risk of loose bodies (i.e., pinheads) in the joint, previous work with these pins has shown via India ink staining that the pins do not cause any damage or defects on the opposing patellar surface[16].

Picrosirius red and safranin O/fast green stainings were performed to gain insight into the composition of the repair cartilage within the cartilage defects (Figures 7B and 8)[32]. Across all of the animals and experimental groups, variability in repair tissue staining and morphology was observed. Generally, the fixation of composites with fibrin glue resulted in more intense picrosirius red staining than fixation with pins, indicating increased collagen formation

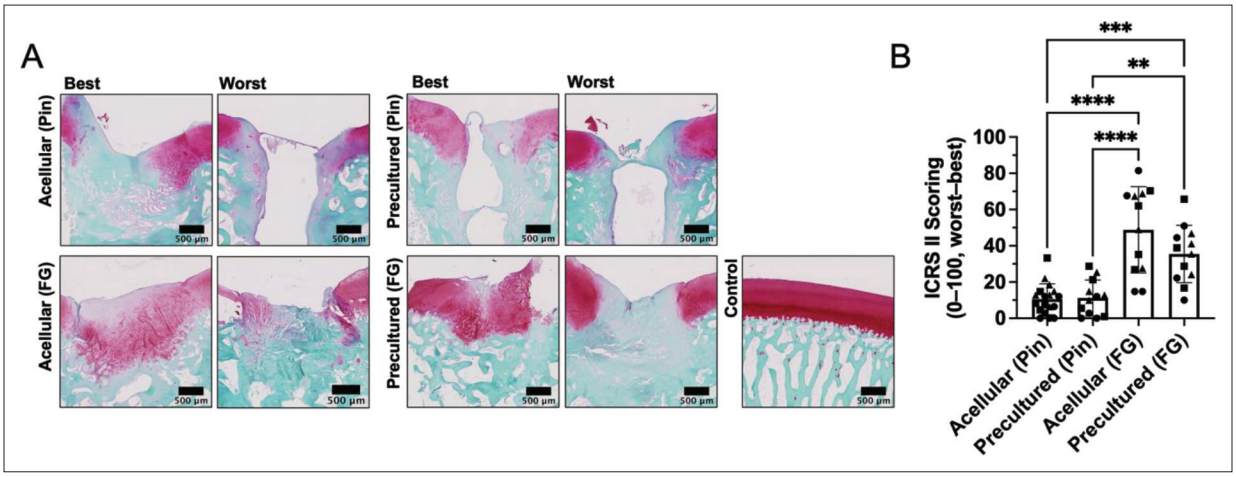

Figure 8. Evaluation of implant fixation methods via safranin O/fast green staining. (A) Safranin O/fast green staining of repair cartilage, with representative cross-sectional images showing the center of cartilage defects for each of the respective experimental groups 12 weeks after composite implantation. Control osteochondral samples were isolated from the most distal portion of the trochlea for qualitative comparisons. Scale bars = 500 µm. (B) ICRS II scoring of repair cartilage by 3 blinded reviewers on a scale of 0–100 (worst–best), where each symbol (circle, square, and triangle) corresponds to scores from each reviewer. $n \geq 12$, one-way ANOVA with Tukey's HSD *post-hoc* test, $^{**}p < 0.01$, $^{***}p < 0.001$, $^{****}p < 0.0001$. FG: fibrin glue.

within defects. In addition, picrosirius red staining revealed that fibrin glue-fixed composites exhibited improved defect filling over pinned composites. However, only marginal differences in picrosirius red staining intensity and tissue morphology were observed when comparing acellular versus precultured composites. In healthy explanted osteochondral tissues, safranin O and fast green staining was dark and robust, suggesting the abundant presence of both proteoglycans and collagen within the cartilage and bone phases of the tissue (Figure 8A). In some of the fibrin glue-fixed composites, the integration of nascent tissue was visualized with the adjacent healthy tissue. However, pinned acellular and precultured composites exhibited marginal safranin O staining, even directly adjacent to the apparent pinhead. These observations were corroborated by ICRS II histological scoring, which indicated that the fixation of composites with fibrin glue significantly improved the quality of resultant repair cartilage compared to the pin fixation (Figure 8B). When composites were fixed within defects via the application of fibrin glue, the best-performing samples exhibited significant proteoglycan content and distribution, as evidenced by safranin O staining approaching what was observed for control tissues. The safranin O staining intensity was also higher in precultured composites than in acellular composites, suggesting that the formation of nascent tissue prior to implantation via the chondrogenic preculture period may help to mediate repair cartilage maturation. However, tissue morphology consistent with fibrocartilage was observed across all defects[27,32]. In another recent study that employed MEW-reinforced hydrogels as osteochondral implants in an orthotopic large animal model, cell-free implants showed abundant cell ingrowth and similar results as cell-containing implants[43]. Importantly, the degradation of MEW-NorHA composites *in vivo* via hyaluronidase activity may similarly facilitate cell ingrowth, even in acellular composites, such that over time the scaffold is remodeled into *de novo* cartilage[37]. Taken together with our results, we postulated that mechanical stability is more determining for the success of the implant than the presence of cells and/or precultured extracellular matrix.

Finally, the functional properties of repair cartilage formed in treated defects were evaluated via indentation creep testing, which enables the *in situ* mechanical testing of tissues within defects to elucidate the compressive modulus, tensile modulus, and permeability (Figure 9). The average compressive modulus of repair cartilage across all the experimental groups did not exceed 0.4 MPa, suggesting that the repair cartilage possessed inferior mechanical properties when compared to previously reported modulus values for native cartilage[44]. Indentation testing of healthy tissue controls isolated from the most distal region of the lateral trochlear groove (compressive modulus = 2.00 ± 0.64 MPa) confirmed that each treatment group led to only partial restoration of the defect's biomechanical function.

While no statistical differences in compressive modulus were observed between each of the treatment groups, pinned composites, on average, possessed higher compressive moduli than glued composites. However, the elevated compressive moduli observed for pinned acellular and precultured composites may be due to the presence of the pin within the defect. Careful attention was given to

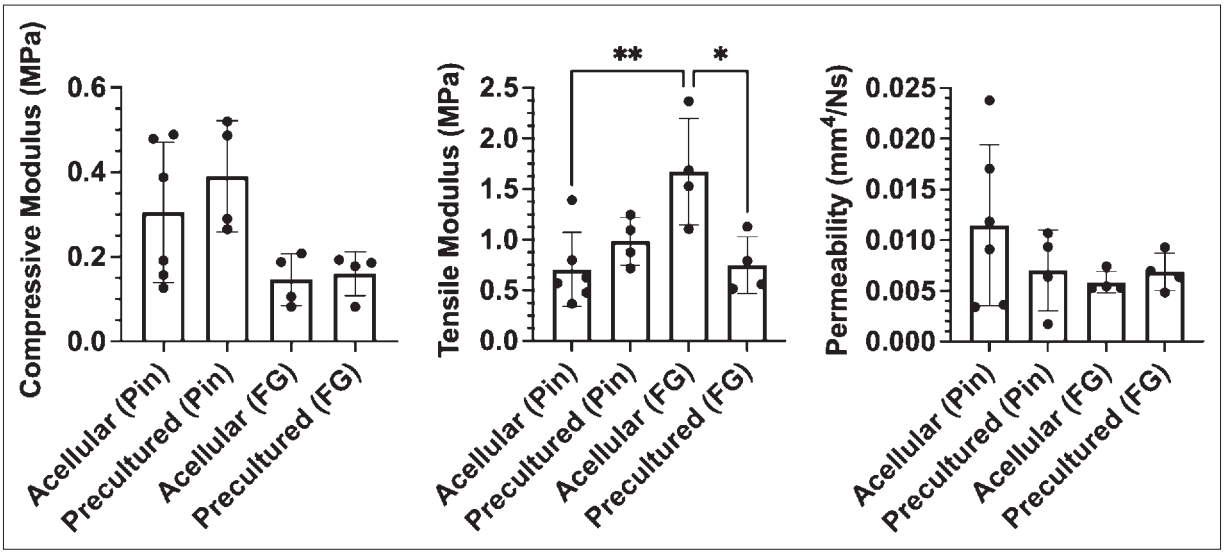

Figure 9. Indentation testing of repair cartilage. Compressive moduli (left), tensile moduli (middle), and permeability (right) of explanted repair cartilage quantified via Hertzian biphasic creep testing 12 weeks after composite implantation. $n \geq 4$, one-way ANOVA with Tukey's HSD *post-hoc* test, $^{*}p < 0.05$, $^{**}p < 0.01$. FG: fibrin glue.

ensure that all indentation tests were performed on tissues adjacent and away from pins to avoid any contribution of the pin to the mechanical properties. Since the pins were also inserted into composites perpendicular to the cartilage surface, it is unlikely that pins were inadvertently underlying tested regions of interest. An alternative source for these observed differences in compressive modulus may be the recruitment of endogenous cells during the formation of pilot holes into the subchondral bone, which could lead to combinations of composite implantation with a single microfracture hole.

In accordance with the tension-compression nonlinearity observed in healthy articular cartilage, the repair cartilage in all of the experimental groups exhibited tensile moduli that were appreciably larger than their respective compressive moduli[45]; however, acellular composites that were implanted with fibrin glue possessed significantly higher tensile moduli than pinned acellular composites and glued precultured composites. Further work would be needed to understand the reason for this. The permeability of repair cartilage across experimental groups is expected to have an inverse relationship with the compressive and tensile moduli, but this trend was only observed for the latter, highlighting the variability of the measured mechanical properties.

Despite the variability in healing response observed across all the experimental groups, when comparing composites only with their baseline properties prior to implantation (Figure 3), the compressive modulus of implanted composites generally increased over time, suggesting delivered and/or endogenous cells mediated the elaboration, maturation, and/or remodeling of nascent repair tissue (Figure 9). An additional important consideration is that the 4 mm defect diameter selected in this model is relatively small (~0.13 cm^2) and within the indicated size range that microfracture would be clinically recommended for a human patient[1]. Therefore, future studies with significantly larger defects may be better suited toward illustrating the composites' potential advantages in repairing defects that would be otherwise challenging to repair (i.e., larger defects approaching or >4 cm^2). Although fibrin glue appears to be more appropriate for the fixation of MEW-NorHA composites in cartilage defects of this size, additional studies are required to validate that the formation of repair cartilage with glued composites is indeed due to successful retention of implants, and not the endogenous repair of an empty defect after implant translocation. In addition, future studies with longer-term time points may better highlight the potential advantages of our composite system over traditional approaches for cartilage defect repair in the clinic.

Taken together, our arthroscopy, micro-CT, histology, and indentation testing demonstrate that further improvements in surgical fixation, overall neocartilage properties, and the animal model selected are needed for a more thorough assessment of MEW-NorHA composites. Both PLDLLA pins and fibrin glue may be used to fix MEW-NorHA composites within full-thickness cartilage defects, albeit with variable success. While retention of samples with fibrin glue may potentially be less reliable than the use of bioresorbable pins, qualitative reductions

in subchondral bone remodeling and improved ECM contents, as evidenced by picrosirius red and safranin O/fast green staining, suggest that future approaches for cartilage repair with MEW-reinforced hydrogels should leverage fibrin glue over pins. To this end, the composite design may be further improved to increase the prospects of this approach. Namely, improved fixation and integration of chondral-only defects may be achieved through the incorporation of tissue-adhesive hydrogels[46,47], while the chondrogenic potential of adult pMSCs may be augmented via coculture with chondrocytes, the presentation of signaling cues that recapitulate the cell–cell interactions present during mesenchymal condensation (i.e., N-cadherin mimetic peptide HAVDI), or the sustained delivery of growth factor such as TGF-β3 *in vivo*[48-50].

4. Conclusion

Previously developed composites of NorHA hydrogels reinforced with melt electrowritten PCL scaffolds were successfully translated to preclinical application with adult porcine MSCs that exhibited viability, chondrogenesis, and cartilage formation during culture. Further, fixation methods and the capacity of MEW-NorHA composites to facilitate the repair of cartilage within full-thickness chondral defects were evaluated. Despite their ability to form neocartilage *in vitro* with multiple porcine donors, composites with chondrogenic preculture did not exhibit any marked improvements in terms of the quality of cartilage form when compared to acellular composites, supporting the hypothesis that the underlying drive for cartilage ECM formation in these smaller defects is the mechanical environment, rather than the transplantation of chondrogenic cells. While the use of PLDLLA pins appears to have ensured the retention of most composites within defects, the size of the pins relative to the defect size may have compromised the ability of repair tissue to fill defects completely. Moreover, the loading imparted by the pinning process itself could have adversely impacted the outcomes of pinned composite groups by compromising the mechanical properties of composites and/or contracting the composites, causing them to sink in defects and poorly integrate with peripheral tissue. In contrast, fixation of composites with fibrin glue led to the repair of cartilage with improved gross appearance and more complete defect filling. These results will guide future *in vivo* assessments of MEW-reinforced hydrogels employed for cartilage or orthopedic tissue engineering applications.

Acknowledgments

The authors would like to thank Robert Spiro from Aesculap Biologics for kindly donating the bioresorbable pins employed in this study. The authors also thank Penn University Laboratory Animal Resources (ULAR) for their assistance with the performed animal studies, the Penn Center for Musculoskeletal Disorders (PCMD) for assistance with mechanical testing, Sanjana Hemdev for assistance with processing micro-CT images, and both Elizabeth Henning and Jay Patel for helpful discussions. The primary antibodies against collagen type II (II-II6B3) developed by T. F. Linsenmayer were obtained from the Developmental Studies Hybridoma Bank, developed under the auspices of the NICHD of the NIH, and maintained by the University of Iowa, Department of Biology (Iowa City, IA, USA).

Funding

This work received financial support from the AO Foundation through the Osteochondral Defect Collaborative Research Program (AO-OCD Consortium TA1711481: Osteochondral Bone Repair with Innovative Tissue Engineering and 3D Bioactive Composite Scaffold), the National Science Foundation (graduate research fellowship to JHG), the National Institute of Health (R01 AR077362, F31 AR077395, P30 AR069619, T32 AR053461), and the US Department of Veterans' Affairs (IK6 RX003416, IK1 RX003932). JM and RL acknowledge support from the Dutch Arthritis Society (LLP-12 and LLP-22) and the Gravitation Program "Materials Driven Regeneration" funded by the Netherlands Organization for Scientific Research (024.003.013).

Conflict of interest

The authors declare no conflict of interests.

Author contributions

Conceptualization: Jonathan Galarraga, Robert Mauck, Jason Burdick

Formal analysis: Jonathan Galarraga, Hannah Zlotnick, Ryan Locke

Investigation: Jonathan Galarraga, Hannah Zlotnick, Ryan Locke, Sachin Gupta, Natalie Fogarty, Kendall Masada, Brendan Stoeckl, Lorielle Laforest

Writing – original draft: Jonathan Galarraga

Writing – review & editing: Miguel Castilho, Jos Malda, Riccardo Levato, James Carey, Robert Mauck, Jason Burdick

Ethics approval and consent to participate

All the performed animal procedures were approved by the Institutional Animal Care and Use Committee (IACUC) at the University of Pennsylvania (Protocol number 805077).

Consent for publication

Not applicable.

Availability of data

All reported data are available upon reasonable request to the corresponding authors.

References

1. Kalson NS, Gikas PD, Briggs TWR, 2010, Current strategies for knee cartilage repair. *Int J Clin Pract*, 64(10): 1444–1452.

   https://doi.org/10.1111/j.1742-1241.2010.02420.x

2. Everhart JS, Abouljoud MM, Flanigan DC, 2019, Role of full-thickness cartilage defects in knee osteoarthritis (OA) incidence and progression: Data from the OA Initiative. *J Orthop Res*, 37(1): 77–83.

   https://doi.org/10.1002/jor.24140

3. Carey JL, 2012, Fibrocartilage following microfracture is not as robust as native articular cartilage. *J Bone Joint Surg*, 94(11): e80.

   https://doi.org/10.2106/JBJS.L.00319

4. Martín AR, Patel JM, Zlotnick HM, *et al*., 2019, Emerging therapies for cartilage regeneration in currently excluded 'red knee' populations. *NPJ Regen Med*, 4(12): 1–11.

   https://doi.org/10.1038/s41536-019-0074-7

5. Johnstone B, Stoddart MJ, Im GI, 2020, Multi-disciplinary approaches for cell-based cartilage regeneration. *J Orthop Res*, 38(3): 463–472.

   https://doi.org/10.1002/jor.24458

6. Bothe F, Deubel AK, Hesse E, *et al*., 2019, Treatment of focal cartilage defects in minipigs with zonal chondrocyte/mesenchymal progenitor cell constructs. *Int J Mol Sci*, 20(3): 1–17.

   https://doi.org/10.3390/ijms20030653

7. Diloksumpan P, Abinzano F, de Ruijter M, *et al*., 2021, The complexity of joint regeneration: How an advanced implant could fail by its in vivo proven bone component. *J Trial Error,* 2(1): 1–20.

   https://doi.org/10.36850/e3

8. Mancini IAD, Schmidt S, Brommer H, *et al*., 2020, A composite hydrogel-3D printed thermoplast osteochondral anchor as example for a zonal approach to cartilage repair: In vivo performance in a long-term equine model. *Biofabrication*, 12(3): 035028.

   https://doi.org/10.1088/1758-5090/ab94ce

9. Sennett ML, Friedman JM, Ashley BS, *et al*., 2021, Long term outcomes of biomaterial -mediated repair of focal cartilage defects in a large animal model. *Eur Cell Mater*, 41: 40–51.

   https://doi.org/10.22203/eCM.v041a04

10. Chu CR, Szczodry M, Bruno S, 2010, Animal models for cartilage regeneration. *Tissue Eng Part B Rev*, 16(1): 105–115.

    https://doi.org/10.1089=ten.teb.2009.0452

11. Ahern BJ, Parvizi J, Boston R, *et al*., 2009, Preclinical animal models in single site cartilage defect testing: A systematic review. *Osteoarthr Cartil*, 17(6): 705–713.

    https://doi.org/10.1016/j.joca.2008.11.008

12. Mancini IAD, Vindas Bolaños RA, Brommer H, *et al*., 2017, Fixation of hydrogel constructs for cartilage repair in the equine model: A challenging issue. *Tissue Eng Part C Methods*, 23(11): 804–814.

    https://doi.org/10.1089/ten.tec.2017.0200

13. Gotterbarm T, Breusch SJ, Schneider U, *et al*., 2008, The minipig model for experimental chondral and osteochondral defect repair in tissue engineering: Retrospective analysis of 180 defects. *Lab Anim*, 42(1): 71–82.

    https://doi.org/10.1258/la.2007.06029e

14. Drobnič M, Radosavljevič D, Ravnik D, *et al*., 2006, Comparison of four techniques for the fixation of a collagen scaffold in the human cadaveric knee. *Osteoarthr Cartil*, 14(4): 337–344.

    https://doi.org/10.1016/j.joca.2005.11.007

15. Duchow J, Hess T, Kohn D, 2000, Primary stability of press-fit-implanted osteochondral grafts: influence of graft size, repeated insertion, and harvesting technique. *Am J Sports Med*, 28(1): 24–27.

    https://doi.org/10.1177/03635465000280011601

16. Patel JM, Sennett ML, Martin AR, *et al*., 2020, Resorbable pins to enhance scaffold retention in a porcine chondral defect model. *Cartilage,* 13(2): 1676S–1687S.

    https://doi.org/10.1177/1947603520962568

17. Efe T, Füglein A, Heyse TJ, *et al*., 2012, Fibrin glue does not improve the fixation of press-fitted cell-free collagen gel plugs in an ex vivo cartilage repair model. *Knee Sur Sports Traumatol Arthrosc*, 20(2): 210–215.

    https://doi.org/10.1007/s00167-011-1571-4

18. Friedman JM, Sennett ML, Bonadio MB, *et al*., 2018, Comparison of fixation techniques of 3D-woven poly(∈-Caprolactone) scaffolds for cartilage repair in a weightbearing porcine large animal model. *Cartilage*, 9(4): 428–437.

    https://doi.org/10.1177/1947603517700953

19. Hunziker EB, Stähli A, 2008, Surgical suturing of articular cartilage induces osteoarthritis-like changes. *Bone*, 23(1): 1–7.

    https://doi.org/10.1016/j.joca.2008.01.009

20. Vikingsson L, Sancho-Tello M, Ruiz-Saurí A, *et al*., 2015, Implantation of a polycaprolactone scaffold with subchondral bone anchoring ameliorates nodules formation and other tissue alterations. *Int J Artif Organs*, 38(12): 659–666.

    https://doi.org/10.5301/ijao.5000457

21. Galarraga JH, Locke RC, Witherel CE, *et al*., 2022, Fabrication of MSC-laden composites of hyaluronic acid hydrogels reinforced with MEW scaffolds for cartilage repair. *Biofabrication*, 14(1): 014106.

    https://doi.org/10.1088/1758-5090/ac3acb

22. Castilho M, Hochleitner G, Wilson W, *et al*., 2018, Mechanical behavior of a soft hydrogel reinforced with three-dimensional printed microfibre scaffolds. *Sci Rep*, 8(1): 1245.

    https://doi.org/10.1038/s41598-018-19502-y

23. Galarraga JH, Kwon MY, Burdick JA, 2019, 3D bioprinting via an in situ crosslinking technique towards engineering cartilage tissue. *Sci Rep*, 9(1): 19987.

    https://doi.org/10.1038/s41598-019-56117-3

24. Kim M, Erickson IE, Choudhury M, *et al*., 2012, Transient exposure to TGF-β3 improves the functional chondrogenesis of MSC-laden hyaluronic acid hydrogels. *J Mech Behav Biomed Mater*, 11: 92–101.

    https://doi.org/10.1016/j.jmbbm.2012.03.006

25. Kwon MY, Vega SL, Gramlich WM, *et al*., 2018, Dose and timing of N-cadherin mimetic peptides regulate MSC chondrogenesis within hydrogels. *Adv Healthc Mater*, 7(9): 1701199.

    https://doi.org/10.1002/adhm.201701199

26. Zlotnick HM, Locke RC, Stoeckl BD, *et al*., 2021, Marked differences in local bone remodelling in response to different marrow stimulation techniques in a large animal. *Eur Cell Mater*, 41: 546–557.

    https://doi.org/10.22203/eCM.v041a35

27. Fisher MB, Belkin NS, Milby AH, *et al*., 2015, Cartilage repair and subchondral bone remodeling in response to focal lesions in a mini-pig model: Implications for tissue engineering. *Tissue Eng Part A*, 21(3–4): 850–860.

    https://doi.org/10.1089/ten.tea.2014.0384

28. Collins D, Simons B, 2020, Significantly delayed polyglactin 910 suture-related pseudoinfection in a yucatan pig. *BMC Vet Res*, 16(1): 1–7.

    https://doi.org/10.1186/s12917-020-02662-3

29. Smith G, Taylor J, Almqvist KF, *et al*., 2005, Arthroscopic assessment of cartilage repair: A validation study of 2 scoring systems. *Arthroscopy*, 21(12): 1462–1467.

    https://doi.org/10.1016/j.arthro.2005.09.007

30. Goebel L, Orth P, Müller A, *et al*., 2012, Experimental scoring systems for macroscopic articular cartilage repair correlate with the MOCART score assessed by a high-field MRI at 9.4 T - comparative evaluation of five macroscopic scoring systems in a large animal cartilage defect model. *Osteoarthr Cartil*, 20(9): 1046–1055.

    https://doi.org/10.1016/j.joca.2012.05.010

31. Erickson IE, Kestle SR, Zellars KH, *et al*., 2012, Improved cartilage repair via in vitro pre-maturation of MSC-seeded hyaluronic acid hydrogels. *Biomed Mater*, 7(2): 024110.

    https://doi.org/10.1088/1748-6041/7/2/024110

32. Mainil-Varlet P, Van Damme B, Nesic D, *et al*., 2010, A new histology scoring system for the assessment of the quality of human cartilage repair: ICRS II. *Am J Sports Med*, 38(5): 880–890.

    https://doi.org/10.1177/0363546509359068

33. Stoeckl BD, Zlotnick HM, Farrell MJ, *et al*., 2021, The porcine accessory carpal bone as a model for biologic joint replacement for trapeziometacarpal osteoarthritis. *Acta Biomater*, 129: 159–168.

    https://doi.org/10.1016/j.actbio.2021.05.011

34. Patel JM, Wise BC, Bonnevie ED, *et al*., 2019, A systematic review and guide to mechanical testing for articular cartilage tissue engineering. *Tissue Eng Part C Methods*, 25(10): 593–608.

    https://doi.org/10.1089/ten.tec.2019.0116

35. Moore AC, DeLucca JF, Elliott DM, *et al*., 2016, Quantifying cartilage contact modulus, tension modulus, and permeability with hertzian biphasic creep. *J Tribol*, 138(4): 1–7.

    https://doi.org/10.1115/1.4032917

36. Fisher MB, Belkin NS, Milby AH, *et al*., 2016, Effects of mesenchymal stem cell and growth factor delivery on cartilage repair in a mini-pig model. *Cartilage*, 7(2): 174–184.

    https://doi.org/10.1177/1947603515623030

37. Galarraga JH, Dhand AP, Enzmann BP, *et al*., 2023, Synthesis, characterization, and digital light processing of a hydrolytically degradable hyaluronic acid hydrogel. *Biomacromolecules*, 24(1): 413–425.

    https://doi.org/10.1021/acs.biomac.2c01218

38. Qayed M, Copland I, Galipeau J, 2017, *Allogeneic Versus Autologous Mesenchymal Stromal Cells and Donor-To-Donor Variability*. Elsevier Inc, Amsterdam.

    https://doi.org/10.1016/b978-0-12-802826-1.00004-0

39. Pfeifer CG, Fisher MB, Saxena V, *et al*., 2017, Age-dependent subchondral bone remodeling and cartilage repair in a minipig defect model. *Tissue Eng Part C Methods*, 23(11): 745–753.

    https://doi.org/10.1089/ten.tec.2017.0109

40. Brittberg M, Winalski CS, 2003, Evaluation of cartilage injuries and repair. *J Bone Joint Surg Series A*, 85(2): 58–69.

    https://doi.org/10.2106/00004623-200300002-00008

41. Mithoefer K, Mcadams T, Williams RJ, *et al*., 2009, Clinical efficacy of the microfracture technique for articular cartilage repair in the knee: An evidence-based systematic analysis. *Am J Sports Med*, 37(10): 2053–2063.

    https://doi.org/10.1177/0363546508328414

42. Donell S, 2019, Subchondral bone remodelling in osteoarthritis. *EFORT Open Rev*, 4(6): 221–229.

https://doi.org/10.1302/2058-5241.4.180102

43. de Ruijter M, Diloksumpan P, Dokter I, *et al*., 2022, Pivotal importance of reinforcement of cartilage implants confirmed in challenging large animal model; presence of transplanted cells probably secondary, in *Tissue Engineering Part A*, Mary Ann Liebert, Inc., USA, S289–S290.

44. Mansour JM, 2009, Biomechanics of Cartilage. In: Lupash EJ, Klingler AM, Glover SA, eds. *Kinesiology: The Mechanics and Pathomechanics of Human Movement*. Second. Lippincott Williams & Wilkins, Philadelphia, 69–81.

45. Huang CY, Mow VC, Ateshian GA, 2001, The role of flow-independent viscoelasticity in the biphasic tensile and compressive responses of articular cartilage. *J Biomech Eng*, 123(5): 410–417.

https://doi.org/10.1115/1.1392316

46. Zhang X, Jiang Y, Han L, *et al*., 2021, Biodegradable polymer hydrogel-based tissue adhesives: A review. *Biosurf Biotribol*, 7(4): 163–179.

https://doi.org/10.1049/bsb2.12016

47. Nam S, Mooney D, 2021, Polymeric tissue adhesives. *Chem Rev*, 121(18): 11336–11384.

https://doi.org/10.1021/acs.chemrev.0c00798

48. Kim M, Steinberg DR, Burdick JA, *et al*., 2019, Extracellular vesicles mediate improved functional outcomes in engineered cartilage produced from MSC/chondrocyte cocultures. *Proc Natl Acad Sci USA*, 116(5): 1569–1578.

https://doi.org/10.1073/pnas.1815447116

49. Vega SL, Kwon MY, Song KH, *et al*., 2018, Combinatorial hydrogels with biochemical gradients for screening 3D cellular microenvironments. *Nat Commun*, 9: 614.

https://doi.org/10.1038/s41467-018-03021-5

50. Patel JM, Saleh KS, Burdick JA, *et al*., 2019, Bioactive factors for cartilage repair and regeneration: Improving delivery, retention, and activity. *Acta Biomater*, 93: 222–238.

https://doi.org/10.1016/j.actbio.2019.01.061